Vol. 189: 77–92, 1999 | MARINE ECOLOGY PROGRESS SERIES Mar Ecol Prog Ser | Published November 26

'Phyto-convection': the role of oceanic convection in primary production

Jan O. Backhaus[1,*], Henning Wehde[1], Else Nøst Hegseth[2], Jochen Kämpf[3]

[1] Institute of Oceanography, University of Hamburg, Troplowitzstr 7, 22529 Hamburg, Germany
[2] The Norwegian College of Fisheries Science, University of Tromsø, 9037 Tromsø, Norway
[3] Flinders University, School of Earth Sciences, Adelaide, GPO Box 2100, 5001 South Australia, Australia

ABSTRACT: Typical sinking rates of marine phytoplankton cover a range extending from a few meters up to several hundred meters per day. If it were not for a process which maintains plankton near the sea surface, in the euphotic layer, it would sink to depths of thousands of meters in the deep ocean during the winter season. Consequently, plankton would not be available for the next spring bloom. In shelf seas and coastal areas, as well as in fjords, deep sinking is prohibited by the proximity of the sea bed. The mechanism which reliably initiates a spring bloom is generally not considered in models of marine primary production. Such models generally rely on the assumption that a very small background concentration of plankton is available to initiate a bloom. Penetrative oceanic convection in the open ocean forms the perennial thermocline in winter in mid and high latitudes. The thermocline is situated at depths of several hundred meters. On a shelf, or in a fjord, convection may penetrate to the seabed, thereby affecting the entire water column. We argue that oceanic convection in winter accounts for the availability of plankton in the euphotic layer in spring. In support of this hypothesis a coupled phytoplankton convection model was developed. In this model plankton, i.e. resting spores and vegetative cells, is simulated by Lagrangian tracers moving within the flow predicted by the convection model. For each tracer a simple phytoplankton model predicts growth dependent on light conditions. Plankton spores sink with a prescribed velocity of 120 m d^{-1}. Growing vegetative cells have a sinking rate of only 1 m d^{-1} The model operates in a vertical ocean slice covering the water column. The width of the slice is typically 1 to 3 km, and it is resolved by an isotropic grid size of 5 m. The phyto-convection model was applied to a region in the Barents Sea shelf and to a coastal fjord in the north of Norway. It was run over winter/spring periods under realistic meteorological forcing. Tracers representing resting spores were initially introduced into a thin bottom layer of the model domain, which constitutes the worst case in terms of maximum sinking. The water column, apart from the bottom layer, was assumed to be void of plankton. In both cases convection eroded the initial stratification and dispersed plankton over the entire water column. The onset of a phytoplankton bloom coinciding with the establishment of a (weak) seasonal thermocline in spring was predicted, which agrees with observations from both regions considered. The simulations support the hypothesised role of oceanic convection in primary production.

KEY WORDS: Oceanic convection · Primary production · Dispersion of phytoplankton

INTRODUCTION

Phytoplankton spring blooms normally require a stable surface mixed layer to develop. The mixed layer may either be built up by thermal heating of water masses in the open ocean, and/or by fresh water input in near-shore regions. In northern Norwegian fjords and coastal areas such blooms have long been known to take place in apparently unstratified, or only weakly stratified water masses since strong pycnoclines are not established until May/June, when water temperature and fresh water input increase (Heimdal 1974, Eilertsen & Taasen 1984, Hegseth et al. 1995).

Although spring blooms have been studied extensively during the past 25 yr, the initialisation of a bloom has (surprisingly) received less attention. New investigations have demonstrated the probability of diatom resting spores functioning as the bloom inoculum (Eilertsen et al. 1995, Hegseth et al. 1995) and thereby playing an essential role in phytoplankton population

*E-mail: backhaus@dkrz.de

dynamics. The idea that resuspended resting spores act as seed populations for blooms was presented by Gran (1912). He considered spores as an overwintering stage, but later studies have shown that they may have a wider range of functions and seed blooms on variable time scales and in variable ecological systems (Garrison 1984, Smetacek 1984, Pitcher 1991, Pitcher et al. 1992). In temperate areas it has proven difficult to verify that spores actually seed the spring bloom since vegetative cells are always present during winter (Garrison 1981, 1984). However, in northern Norway the winter situation is characterised by a long dark period with extremely low phytoplankton biomass. The few vegetative cells present do not belong to the spring bloom species (Hegseth et al. 1995, von Quillfeldt 1996); rather they represent benthic populations and thereby indicate resuspension from the bottom. Hence, the inoculum for the spring bloom has to come from somewhere other than from the water masses, and resting spores are the most likely source. The soft sediment surface of northern Norwegian fjords contains large amounts of spores which have been shown to germinate and develop into a spring bloom under experimental conditions (Eilertsen et al. 1995).

Typical sinking rates of marine phytoplankton, mostly diatoms, cover a wide range from a few meters up to several hundred meters per day (Smayda 1970, von Bodungen et al. 1981, Billett et al. 1983, Platt et al. 1983, Passow 1991). Cells might sink during a winter season to depths of thousands of meters in the deep ocean and consequently would not be available for the next spring bloom. Chlorophyll-containing phytoplankton cells have in fact been reported from depths down to 4300 m (Kimball et al. 1963), indicating high sinking rates. In shelf seas and coastal areas, as well as in fjords, deep sinking is prohibited by the proximity of the seabed. There must, however, be processes which bring up and maintain phytoplankton near the sea surface both in open ocean and in near-shore areas. The physical mechanism which initiates a plankton bloom is generally not considered in detail in models of marine primary production (Aksnes & Lie 1990, Moll 1995). These models rely on the assumption that a very small background concentration of plankton is always available to initiate a spring bloom. Observations appear to justify this assumption, but the actual mechanism which accounts for the presence of plankton in the euphotic layer in spring is still unknown. Barkmann & Woods (1996) simulated a vertical migration of plankton by means of a Monte Carlo approach in which estimates of ambient turbulence (caused by wind and waves) were determined from a turbulence closure scheme. Their Lagrangian study was confined to the upper 200 m of the water column, and they did not try to explain dispersion of plankton during the winter spring season. Several mechanisms have been suggested to bring spores up from the bottom layers to the euphotic zone, turbulent mixing (Eilertsen et al. 1995) or upwelling (Malone et al. 1983, Pitcher 1991) being the most common.

We propose that convection is the mechanism which accounts for the transport of spores to the upper layers during winter and in the early phase of a spring bloom. Convection in high and mid latitudes is driven by a cooling of the sea surface in winter. It is only recently (i.e. in the past 10 to 15 yr) that convection in the ocean has been studied in detail because of its importance as a process relevant for understanding climate dynamics. A comprehensive overview of the present knowledge about oceanic convection, comprising observations and model simulations, is given by Marshall & Schott (1999). Generally, a distinction is made between convection in the open water column and bottom arrested slope convection (also called: cascading). Detailed studies of oceanic convection in the open water column of the Greenland Sea, in the presence of sea ice, were conducted by Backhaus (1995), Backhaus & Kämpf (1999), and Kämpf & Backhaus (1998). Convection in the water column of polar shelves plays an important role in forming dense bottom water masses which ultimately cascade down the continental slope and thus account for ventilation of deep water masses in the Arctic Ocean (Aagaard et al. 1985, Aagaard & Carmach 1989, Rudels 1993, Jungclaus et al. 1995, Backhaus et al. 1997). More information about convection in the context of this investigation is given below (see: 'Synopsis' in 'Materials and methods', where our experimental set up is described).

Penetrative open ocean convection, in contrast to wind-induced and tidal dynamics, is a turbulent process which generally is not confined to the marine boundary (Ekman) layers. Oceanic convection in the open ocean, in mid and high latitudes, forms the perennial thermocline during winter. This thermocline may be situated at depths of several hundred meters, i.e. well beneath the surface Ekman layer. In the North Atlantic, for instance, Subpolar Mode Water masses are formed in winter by convection in the vicinity of the polar front (McCartney & Talley 1982, van Aken & Becker 1997). These waters may cover (on a seasonal average) the upper 200 to 600 m of the water column. On a shelf, or in a fjord, convection may penetrate to the seabed, thereby affecting the entire water column.

We argue that convection in winter accounts for the availability of plankton in the euphotic zone in spring. In support of this hypothesis, and due to a lack of observations from winter, a coupled phytoplankton convection model was developed. In this model plankton is simulated by Lagrangian tracers which move within the flow predicted by an oceanic convection

model. For each tracer a simple phytoplankton model is solved, thus predicting the growth of plankton in both time and space. The 'phyto-convection' model was applied to the Barents Sea shelf and to a coastal fjord in northern Norway by considering a winter/spring period under realistic meteorological forcing.

MATERIALS AND METHODS

Observations and data. Temperature and salinity (T,S) data were sampled regularly by CTD casts in fjords and coastal areas of northern Norway by the University of Tromsø (see Norman 1990, 1991, 1992, 1993, or 'Havmiljödata' database on website of UIT/NFH [University of Tromsø, Norges Fiskeri Hoyskole]). In this work we have used CTD observations from 1990–1995 from Balsfjord. For a shelf region in the Barents Sea T,S data predicted by the HAMSOM model of the Barents Sea (HAMSOM: HAMburg Shelf-Ocean Model, Backhaus 1985, Harms 1994) was provided by Harms (pers. com. 1998). Six-hourly meteorological data (wind speed, air temperature, humidity, and cloudiness), provided by the Norwegian Meteorological Institute (NMI) and the ECMWF (European Centre for Medium Range Weather Forecast), were used as model forcing.

The coupled Phytoplankton-Convection Model (PCM). The main purpose of this modelling process study was to support our hypothesised relationship between oceanic convection and phytoplankton succession and its important contribution to the success of a spring bloom. In addressing this interesting interdisciplinary problem, we hope that this paper will be read by both marine physicists as well as marine biologists. However, disciplines have their specific jargon, in particular when it comes to modelling. We want to avoid distracting, by extensive use of (modelling) jargon, readers who simply want to be informed about the process which we call 'phyto-convection'. We have, therefore, included a short synopsis in which information about both convection and our model is provided. In this synopsis we have avoided use of any jargon. It is followed by a more detailed description of the model which would require some knowledge about both modelling and convection.

Synopsis. Convection, in contrast to predominantly horizontal ocean dynamics, is characterised by substantial vertical, both up- and downward, motions (typical extremes of vertical velocities: up to 20 cm s^{-1}). Here, we consider convective dynamics driven by the negative buoyancy of waters at the sea surface which results from a cooling of the ocean. However, convection can also be induced by heating from beneath, as occurs, for instance, in hydro-thermal vents. Spatial scales of convection are generally much smaller, and vertical accelerations are much larger, than for predominantly horizontal flow. This is characteristic of nonhydrostatic dynamics. Unless convection covers a region large enough to feel the effect of the earth's rotation, it occurs on spatial scales which are well below those of baroclinic eddies (< internal Rossby radius of deformation). Nonhydrostatic dynamics require a special approach in modelling which differs from the commonly used hydrostatic models applied for predominantly horizontal flow. (In nonhydrostatic physics [models] both vertical accelerations and velocities play an important role and require an equation of motion for the vertical co-ordinate. This is not the case for hydrostatic physics where vertical velocities are diagnosed from the equation of continuity; the equation of motion for the vertical co-ordinate is omitted.) The convection model utilised in this investigation has previously been applied for simulations of convection in the Greenland Sea. Hence, a well-tested tool was available.

Convection, originating from a cooled ocean surface, is characterised by energetic downward motions. Sinking of these heavier water masses occurs in narrow funnels, or plumes. Conservation of mass requires an upwelling in the vicinity of sinking regions. The upward motion is generally less energetic and occurs on larger spatial scales. The aspect ratio of convection (Kämpf & Backhaus 1998), i.e. the relation between the horizontal separation of plumes and their vertical extent, has been found to be in the order of 1:2.5 (vertical vs horizontal scale). Both downward and upward motion form a 'convective cell' which may have, dependent on ambient turbulence, a more or less well-organised orbital shape.

According to our hypothesis, plankton is dispersed by the orbital motions of convective cells in winter. To simulate this we considered individual water parcels, i.e. Lagrangian tracers, which are moved around by convective dynamics within the water column. Each tracer in our coupled PCM carries a simple phytoplankton model which predicts plankton growth dependent on environmental conditions (light, nutrients, grazers, etc.). Whenever a tracer approaches the euphotic layer near the sea surface, it may receive an amount of light-quanta before it descends again into the oceanic darkness. Therefore, slow plankton growth is expected which would largely depend on the frequency of the cellular motion. This, in turn, depends on the applied meteorological forcing and may cover a wide range of time scales.

The meteorological forcing of the model comprises winds, air temperature and humidity, cloud coverage, and long and short wave radiation. These parameters

are needed to compute (1) the heat (and buoyancy) fluxes which account for the surface cooling/heating, and (2) the light conditions for the phytoplankton model. As a result of the applied forcing the model predicts the temporal evolution of currents and changes in both temperature/salinity (from which the density is computed). The model requires start conditions for both flow and temperature and salinity. The latter may be obtained from observations. An ocean at rest is usually assumed as dynamical initialisation. The model is defined in a vertical ocean slice by ignoring any gradients normal to the slice. Advection of matter, and of water mass properties, from outside the slice is avoided by 'pasting' the lateral boundaries of the slice together. This way, the model domain becomes a self-contained micro-cosmos: disturbances which may, for instance, leave the ocean slice on the right-hand side re-enter the domain via the left-hand side (modellers jargon: 'cyclic boundary conditions').

Details of the coupled PCM. For the dynamical part, i.e. the convection model, we make reference to previously published papers. For convenience, we denote here only the equations for the biological model which is carried around by each tracer.

A nonhydrostatic, rotational convection model (Backhaus 1995, Backhaus & Wehde 1997) was coupled to a Lagrangian phytoplankton model (Wehde 1996). The convection model was previously applied to investigate convection, resulting water mass formation and ice-ocean interactions in the Greenland Sea (Backhaus 1995, Backhaus & Kämpf 1999, Kämpf & Backhaus 1999). The model ignores large-scale advective transports and works on sub-meso spatial scales, i.e. on scales well below the internal Rossby-radius of deformation.

The ocean model: The non-linear Bousinesq equations for an incompressible fluid of the nonhydrostatic, rotational model and further details about its numerical scheme are described in detail in Kämpf & Backhaus (1998). Therefore, only a brief description is given here. The model utilises an equidistant numerical grid (Arakawa C) and grid sizes in the order of meters. In contrast to previous convection studies, which considered the rotational phase of convection (see overview by Marshall & Schott 1999), our grid is isotropic to avoid any distortions of convective dynamics by a non-isotropic grid. The model domain is a vertical ocean slice with vanishing normal gradients of all variables. With a prescribed grid size of 5 m, the model time step, in the applications described below, varied between 5 and 45 s, dependent on convective dynamics. The time step depends on the courant number of the applied explicit numerical advection scheme for both momentum and water mass properties.

Cyclic boundary conditions at the lateral boundaries of the model domain are applied, thereby excluding lateral advection by the large-scale flow. Independent conservation equations for heat and salt are linked to the momentum equations via a non-linear equation of state (UNESCO). The model predicts the spatial and temporal evolution of T,S (density), nonhydrostatic pressure and flow fields from an initial (horizontally homogeneous) temperature and salinity profile. The turbulent eddy viscosity, and diffusivity, in the ocean model are parameterised by a simple diagnostic 1-equation turbulence closure scheme (Kochergin 1987, Backhaus 1995). Coefficients for turbulent exchange of momentum and diffusion of water mass properties are assumed equal. The validity of this concept is confirmed by our previous convection studies (Backhaus & Kämpf 1999, Kämpf & Backhaus 1999). The high spatial and temporal resolution of the model allows us to resolve a good deal of the turbulent spectrum which is usually parameterised in larger scale models. The ocean model is forced with fluxes of momentum and heat computed from bulk formulae (Gill 1982). For the computation of the heat flux, the sea surface temperature (SST), predicted with the model, and prescribed atmospheric data (air temperature, humidity, wind speed, and cloudiness) are used. The thermodynamic forcing comprises sensible and latent heat-fluxes and short and long-wave radiation (Friehe & Schmitt 1976).

The Lagrangian Transport Model: The simulation of the motion of phytoplankton in the vertical ocean slice of the coupled PCM is accomplished by Lagrangian tracers, i.e. marked water parcels which follow convective dynamics. We preferred to use a Lagrangian approach, as opposed to an Eulerian, because it allowed us to follow single tracers in time (and space). This way a process-oriented simulation of the anticipated dispersion of phytoplankton was achieved. Moreover, Eulerian schemes generally suffer from numerical diffusion, which we wanted to avoid in this application. With each newly predicted flow field, i.e. at each model time step, the positions of all Lagrangian tracers were updated. Convective dynamics may change rapidly on small spatial and temporal scales. Any temporal interpolation in a strongly variable flow field might result in erroneous trajectories of tracers. Therefore, a temporal interpolation of flow fields, sampled from the model output with a time step larger than the (dynamical) model time step, was avoided. Note that in coarser scale tracer simulations tracer positions are often updated from flow fields which are interpolated in time. This is only justified if the flow does not vary on both small temporal and spatial scales.

The Phytoplankton Model: In this study we want to pay special attention to the hypothesised fundamental

Table 1. Constants used in the phytoplankton model

Quantity	Symbol	Value	Unit
Optimum light intensity	I_1	46	W m^{-2}
Extinction coefficient	k_0	0.09	m^{-1}
Maximum growth rate of phytoplankton	r_P	1.5	d^{-1}
Sinking velocity of spores	w_s	120	m d^{-1}
Mortality rate	r_M	0.05	d^{-1}
Grazing rate	r_Z	0.5	d^{-1}
Respiration rate	r_R	0.06	d^{-1}
Phosphate half saturation constant	k_S	0.06	Mmol PO_4-P m^{-3}

relationship between oceanic convection and primary production. Therefore, model components were reduced to the most simple case. We made use of the phytoplankton model described by Moll (1995, 1998). We created a process study void of any second-order effects by reducing our model to essential mechanisms only. For this reason a phytoplankton model was used in which the stock of phytoplankton biomass A (mg C m^{-3}) changes in time (t) according to:

$$\frac{\delta A}{\delta t} = A[r_p \min.(r_I, r_N) - r_R - r_M - r_Z] \quad (1)$$

The right-hand terms of Eq. (1) express gross primary production, respiration, mortality and grazing, where r_R, r_M, and r_Z are respiration, mortality and grazing rates, respectively, and r_p is the optimal growth rate for phytoplankton. In our simple model respiration, mortality and grazing are assumed proportional to the phytoplankton stock A. The term min. (r_I, r_N) in Eq. (1) indicates the minimum of variables in brackets. All constants used in this model are given in Table 1 above.

Following Liebig's law the gross primary production is calculated from the minimum of the limitation functions for light r_I, Eq. (2), and nutrients r_N, Eq. (4). We used Steele's (1962) formulation for underwater light intensity I (W m^{-2}) and optimal light intensity (I_1) including photoinhibition as limitation function for light.

$$r_I = \frac{I}{I_1} e^{(1 - I/I_1)} \quad (2)$$

The self-shading effect of phytoplankton is ignored in the model because our interest in phyto-convection ends with the onset of a phytoplankton bloom. Therefore, the available underwater light intensity, Eq. (3), is modelled by the simple relationship:

$$\frac{\delta I(z;t)}{\delta z} = Q\text{swav}(t) \cdot e^{(-k_0 \cdot z)} \quad (3)$$

where the amount of incoming short wave solar radiation Qswav (W m^{-2}), depending on time, latitude, and observed local cloudiness, is calculated after Dobson & Smith (1988). Here, k_0 is the extinction coefficient which describes a background concentration of suspended matter within the water column, and z (m) is the actual water depth at which the estimate for available underwater light intensity is needed. The Michaelis-Menton relationship Eq. (4) is applied to describe a nutrient limitation. However, in our experiments (cf. Table 1) nutrient limitation will have only a small effect because, according to available observations, there are always enough nutrients available until the peak of a phytoplankton bloom (Mann & Lazier 1991, Hegseth 1995). The limitation of nutrients, considered in Eq. (1), is given by the function:

$$r_N = \frac{P}{P + k_s} \quad (4)$$

where k_S is the half-saturation constant, and P (mmol m^{-3}) the available phosphate.

The sinking velocity (w_s) of tracers representing spores was set to a constant rate of 120 m d^{-1}, in order to simulate observed sinking rates of diatom spores (Degens 1968, Hegseth 1995). With the onset of plankton growth a self-induced buoyancy of growing diatoms, i.e. vegetative cells, was simulated by reducing w_s to 1 m d^{-1} (Moll 1995).

Experimental set-up

Experiments with the PCM, simulating different conditions in polar coastal seas were conducted to study phyto-convection in winter and spring. Regions were chosen for which data for an initialisation of T,S properties were available from either observations or larger scale modelling. The first experiment concerned the Balsfjord (water depth: 160 m; latitude: ~69° 30' N) near Tromsø (henceforth indicated by FJORD), the second a region in the south-western Barents Sea (water depth: 240 m; latitude: ~73° N) which remains ice-free during winter (henceforth indicated by SHELF). In this first attempt to understand phyto-convection sup-

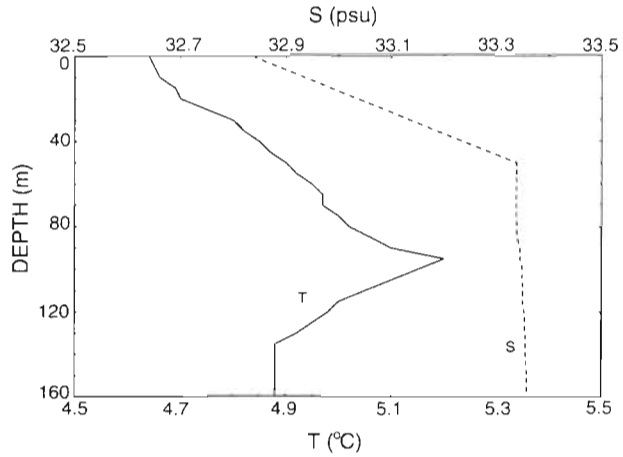

Fig. 1. Observed T,S profile from Balsfjord used for initialisation of Expts FJORD

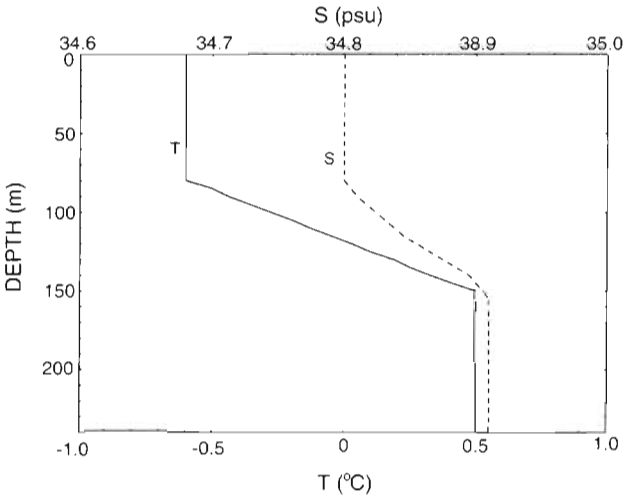

Fig. 2. T,S profile from Barents Sea predicted by HAMSOM Barents Sea model (Harms 1995). This profile was applied for initialisation of Expt SHELF

ported by a process-oriented simulation we wanted to exclude sea ice.

The horizontal dimension of the ocean slice must be chosen to comply with the expected convective aspect ratio, in order to account for a process-oriented spatial resolution of convection. In considering a maximum vertical extent of convection of 160 and 240 m, respectively, i.e. the depth of the considered water columns, we defined a horizontal dimension of 1.25 and 2 km, respectively, for our model domain. With this choice we made sure that at least 3 convection cells were always included within the model domain. The ocean slice was resolved by an isotropic grid size of 5 m.

Two records of 6-hourly meteorological forcing from the years 1990 and 1994 were available for Expt FJORD; for Expt SHELF only data from 1990 were available. Hence, 2 model runs were conducted in the course of Expt FJORD. Both runs were initialised with the same observed T,S profile from Balsfjord (Fig. 1) obtained during winter. The prescribed profile served as initialisation for a process-study conducted with the intention of simulating typical stratification conditions. Making use of one and the same initial stratification allows us to make a judgement on the influence of the meteorological forcing on convection without considering the dependence on different initial conditions. (Our results below show that the final stage of convection in all our experiments is independent of the initial condition, because convection always penetrated through the entire water column, accounting for total homogenisation.)

Expt SHELF was initialised by a T,S profile (Fig. 2) extracted from results of a baroclinic shelf model (Harms 1994, 1995). The latter predicted circulation, water mass, and ice formation for the entire Barents Sea shelf. Its results were validated (Harms 1994) against field observations from Loeng (pers. com. 1996). The T,S profile (Fig. 2) is typical for the ice-free region in the south-western Barents Sea with a dominating influence of the Atlantic inflow.

In all experiments the model was dynamically initialised from a state of rest. With regard to Lagrangian transport the experiments were initialised by a thin (15 m) homogeneous bottom layer in which tracers representing resting spores were evenly distributed. A total of 45 000 tracers was considered in Expt FJORD. In SHELF 67 000 tracers were used, accounting for the larger model domain.

A high number of tracers was chosen to ensure a high resolution in our dispersion study. Based upon our previous experience in convection modelling (Backhaus 1995, Kämpf & Backhaus 1998), we expected a high temporal and spatial variability of tracer distributions as a consequence of the complex convective dynamics. By initially placing all tracers in a thin layer at the seabed, we considered the most extreme case in terms of sinking. This implies that plankton spores had accumulated at the seabed. The water column above the layer was assumed to be void of spores (and vegetative cells). The existence of such a layer can be inferred from observed bottom nepheloid layers which are created within the bottom Ekman layer, for instance, by tidal stirring, or mixing due to internal waves (McCave 1986).

RESULTS

In support of the hypothesised phyto-convection mechanism it is necessary to provide detailed informa-

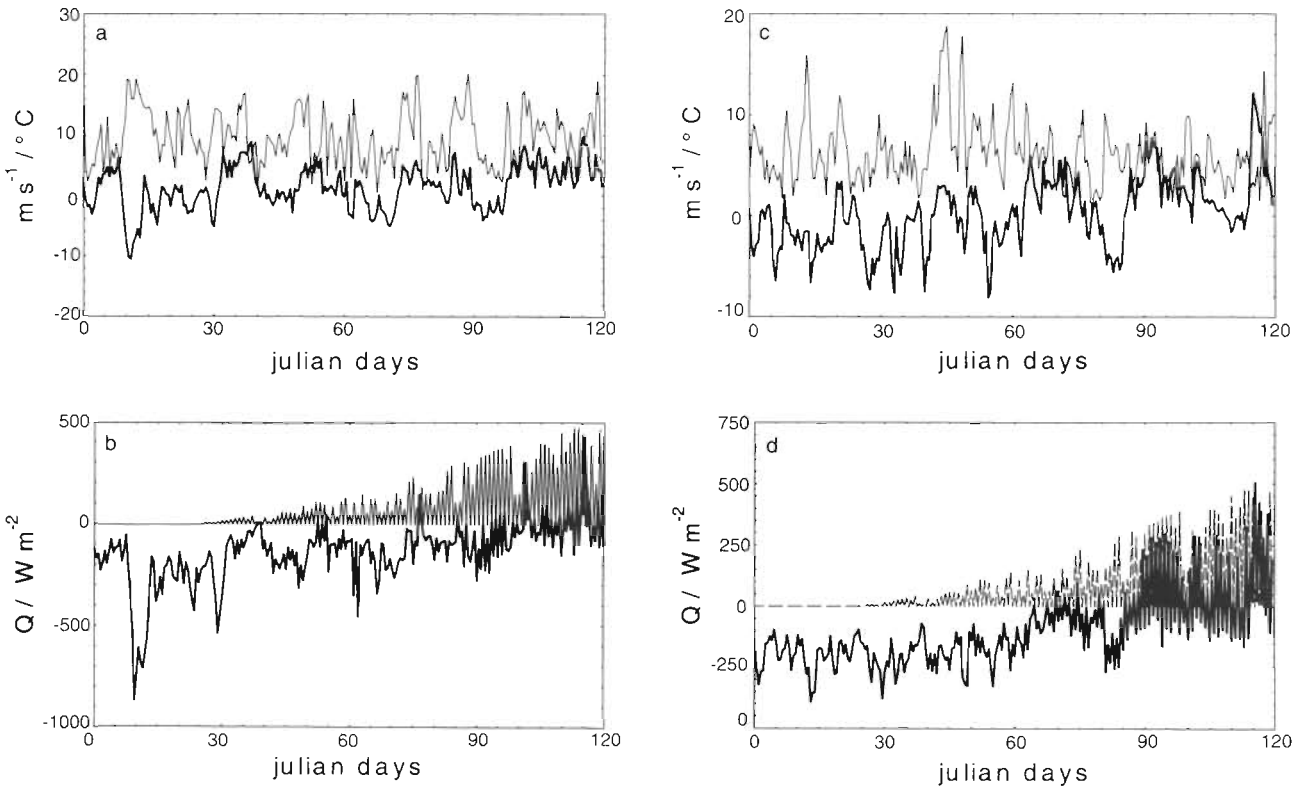

Fig. 3. (a, b) Atmospheric forcing for Expt FJORD 1990. (a) Wind speed (m s^{-1}; thin line) and air temperature (°C; bold line) obtained from ECMWF. (b) Incoming solar radiation (W m^{-2}; thin line) and net heat flux between ocean and atmosphere (W m^{-2}; bold line). Negative values imply heat loss of the water column. (c, d) Atmospheric forcing for Expt FJORD 1994. (c) Wind speed (m s^{-1}; thin line) and air temperature (°C; bold line) obtained from ECMWF. (d) Incoming solar radiation (W m^{-2}; thin line) and net heat flux between ocean and atmosphere (W m^{-2}; bold line). Negative values imply heat loss of the water column

tion about both tracer dispersion and plankton growth during a winter/spring period. Since, in our model, dispersion and growth results from the combined effect of oceanic convection, thermodynamic forcing, and light conditions, we also need to describe the physical environment. A description of the results of our simulations can largely be confined to Expt FJORD because those results also exemplify the results obtained for Expt SHELF. However, the most important information emerging from the latter, i.e. plankton production in relation to the stratification predicted for spring, will be presented.

Meteorological forcing for Expts FJORD and SHELF

Expt FJORD consists of 2 separate model runs, each covering a time span of 120 d. The runs were conducted for 2 different winter/spring seasons (1990 and 1994) in which the model was forced by 6-hourly atmospheric data obtained from the Norwegian Meteorological Institute and the ECMWF. The data (Fig. 3) were chosen because they represent the forcing for a comparatively mild (1994) and a colder winter (1990), respectively. This allows us to judge the dependency of phyto-convection on the applied forcing. For Expt SHELF (Fig. 4), performed in the Barents Sea, only 1 model run with an atmospheric forcing from 1990 was conducted. In Expt SHELF, performed further north, oceanic heat losses during the winter/spring period of 1990 were much higher (Fig. 4b), even as compared with the cold FJORD forcing from 1990 (cf. Fig. 3b).

Expt FJORD

Predicted water mass properties

The evolution of the thermal stratification in Expt FJORD 1990, resulting from convective activity, is given by both a series of consecutive temperature profiles (Fig. 5) and a T,S diagram (see Fig. 7). The forcing for the winter/spring season of 1990 accounted for a rapid cooling of near surface waters which de-stabilised the stratification (Fig. 5a). The final stage of the convective erosion of the initially stable stratified

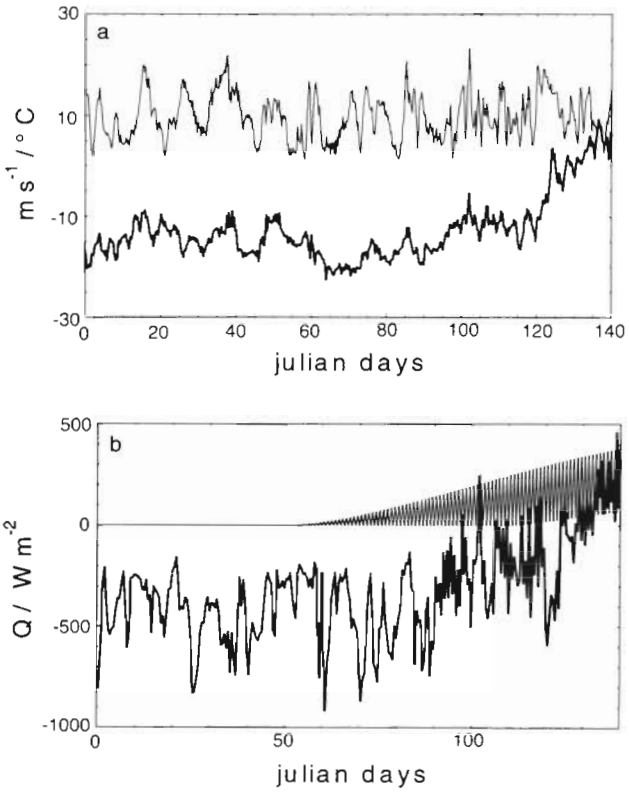

Fig. 4. Atmospheric forcing for Expt SHELF 1990. (a) Wind speed (m s^{-1}; thin line) and air temperature (°C; bold line) obtained from ECMWF. (b) Incoming solar radiation (W m^{-2}; thin line) and net heat flux between ocean and atmosphere (W m^{-2}; bold line). Negative values imply heat loss of the water column

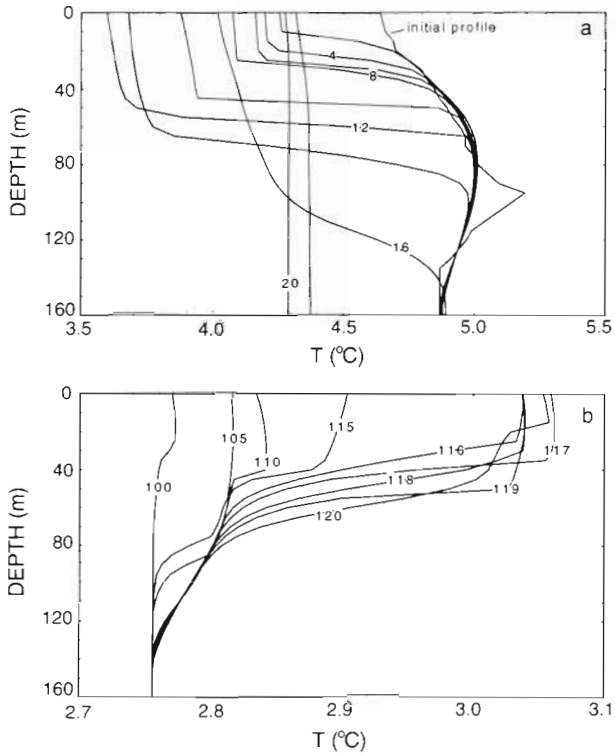

Fig. 5. Predicted evolution of temperature (°C) for Expt FJORD 1990. (a) Simulation time: 0 to 20 d; (b) simulation time: 100 to 120 d. Note differences in scaling the *x*-axis

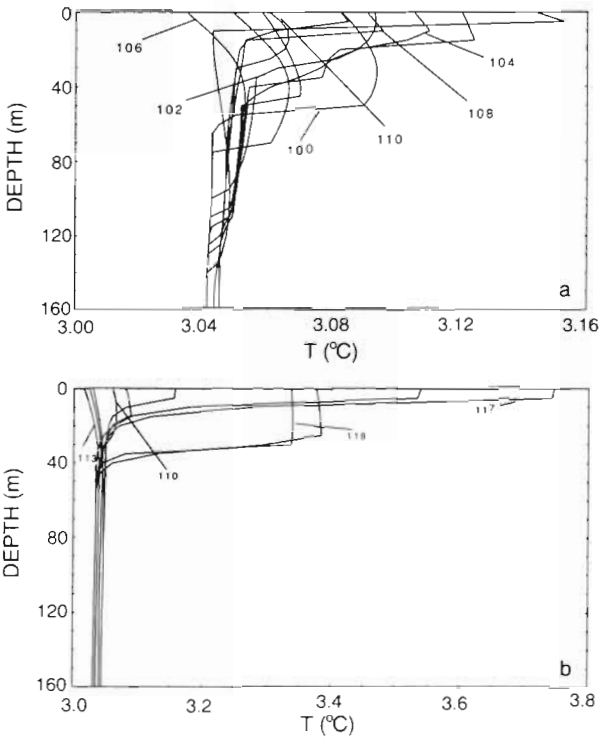

Fig. 6. Predicted evolution of temperature (°C) for Expt FJORD 1994. (a) Simulation time: 100 to 110 d; (b) simulation time: 110 to 120 d. Note differences in scaling the *x*-axis

water column was a total homogenisation of water masses. For spring 1990 (time > Day 100) the onset of a seasonal thermocline was predicted (Fig. 5b).

Temperature profiles from the final simulation days of Expt FJORD 1994 (Fig. 6) show the establishment of a seasonal thermocline similar to that predicted for 1990. However, as a result of the milder forcing, bottom temperatures (Fig. 6) at the end of the winter are higher than those predicted for 1990 (cf. Fig. 5b). For the winter/spring period of 1994 as well convection accounts for the total homogenisation of the water column (not shown).

Convective water mass transformation for both cooling and warming phases are best described in a T,S diagram (Fig. 7). In the diagram for simulation FJORD 1990 a homogenisation of the haline stratification together with a cooling of the upper part of the water column is evident. This is seen from a comparison of the T,S properties at 12 h (close to the initial T,S properties) and the T,S characteristics obtained after 15 d (Fig 7). Thereafter, convection penetrates

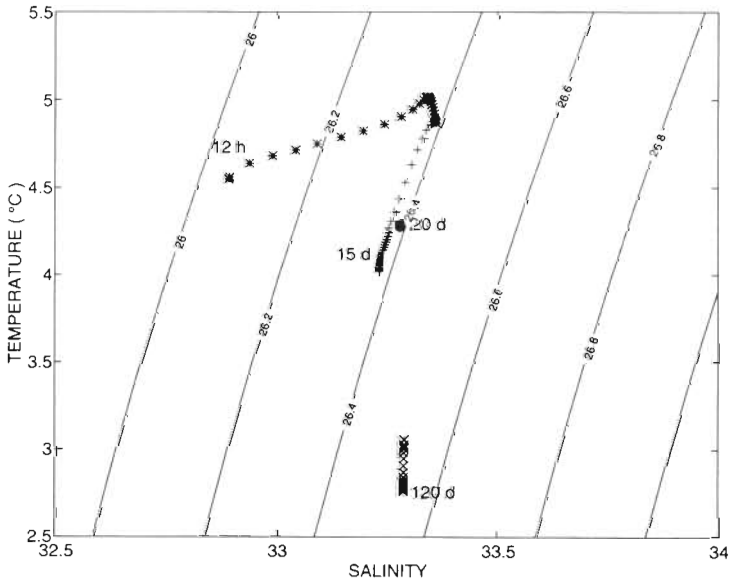

Fig. 7. Predicted convective water mass formation for Expt FJORD 1990. T,S diagrams for selected simulation times as indicated

down to the bottom and, finally, total homogenisation in terms of both temperature and salinity is obtained. The resulting T,S cluster of the homogeneous water mass appears as 1 T,S point (cf. results after 20 d in Fig. 7) with T ~ 4.3°C, and S ~ 33.3 psu. Salinity, in our simulation, behaves like a passive tracer due to the thermal character of convection, as opposed to haline convection which occurs when ice is formed (Backhaus et al. 1997). With an ongoing cooling of the system, for the remaining winter period, the point cluster approaches a minimum temperature at ~2.7°C. The onset of the seasonal thermocline is seen by T,S clusters approaching higher temperatures, starting at the lowest winter temperature (cf. results after 120 d in Fig. 7). The T,S diagram for Expt FJORD 1990 (Fig. 7) is a typical example of a convection which, during winter, penetrated through the entire water column.

The predicted temperature profiles of Expt FJORD may be compared with a typical seasonal cycle of the observed thermal stratification in Balsfjord (Fig. 8). Predicted bottom temperatures at the end of a winter agree very well with the observed temperatures (cf. Figs 5, 6, & 8).

Convection and tracer dispersion

Convective dynamics penetrating towards the seabed, thereby 'collecting' tracers from the thin bottom layer, are depicted by instantaneous temperature contours (Fig. 9) within the ocean slice. Predicted tracer positions are superimposed on the temperature contours to illustrate convective activity. Well before convection has proceeded all the way down to the seabed (time <15 d) the shape of the bottom layer of tracers attains a wavy structure (Fig. 9a,b). These motions near the seabed are driven by nonhydrostatic pressure fluctuations which are generated by convection and transmitted through the water column despite the remaining stratification (Backhaus 1995, Backhaus & Kämpf 1999).

Apparently, convective dynamics also have an influence on dynamics which are well beneath the actual penetration depth of convection. However, soon after simulation Day 16, tracers left the bottom layer and start to move into the water column (Fig. 9c). At first the instantaneous tracer positions remained close together (Fig. 9d), resulting in almost isolated trajectories. However, with time (Days 15 to 25), tracers increasingly covered the entire water column and their distribution (Fig. 9e, f) resembled a marble-like pattern (note that temperature contours were omitted in Fig. 9e,f because of the thermal homogenisation of the water column). Up until ca 40 d of simulation, a thin region near the sea surface remained remarkably free of tracers (Fig. 9e,f). The tracer-free surface layer showed significant changes in thickness. During later stages of the simulation, how-

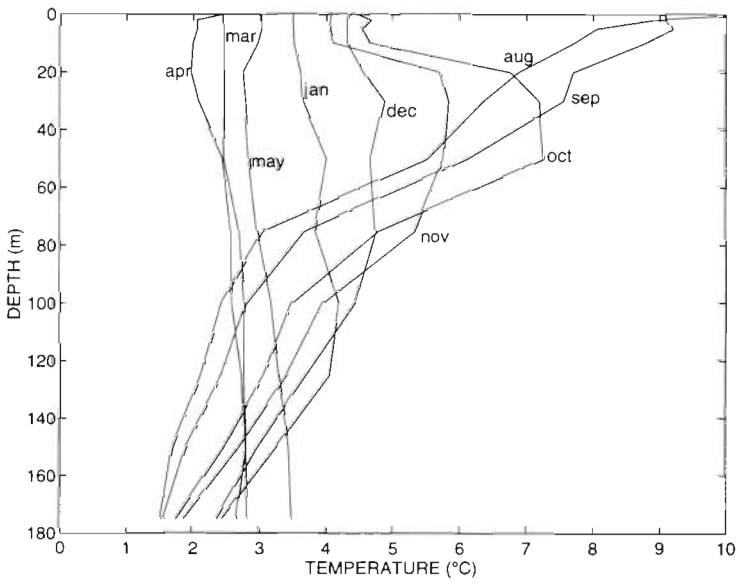

Fig. 8. Typical seasonal cycle of temperature (°C) for Balsfjord/Norway. Observed CTD data at standard depths

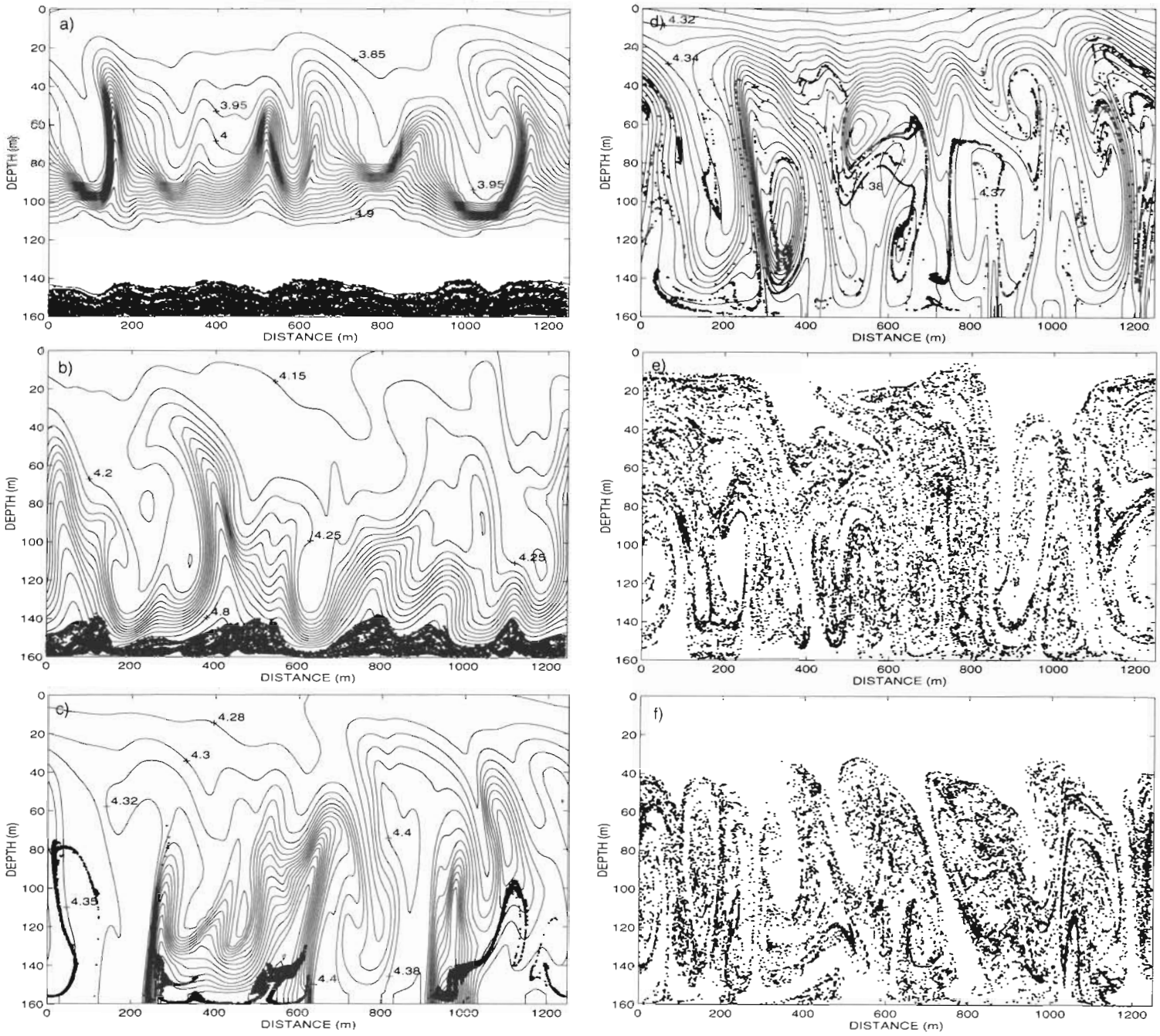

Fig. 9. (a–d) Temperature contours (°C) and tracer distribution in ocean slice for Expt FJORD 1990 after (a) 14 (b) 15.5 (c) 16.5 and (d) 17 d of simulation. (e, f) Tracer distribution in ocean slice for Expt FJORD 1990 after (e) 20 and (f) 21 d of simulation

ever, tracers were also found close to the sea surface (not shown), and a nearly homogeneous distribution within the entire water column was obtained.

Fig 10 illustrates orbital motions of 2 selected tracers during 100 h of simulation starting at Day 16.5. It is evident that the trajectories are better described as being more like a drunkard's walk rather than a well-defined orbital cell. This is caused by ambient turbulence which is induced by convection itself. The final fate of 2 other tracers, randomly selected from the ocean slice, is illustrated by time series of their vertical positions (Fig. 11) for the entire simulation. With decaying convective activity, which coincides with the establishment of a seasonal thermocline (cf. Fig. 5b), vertical displacements of tracers become very small. One tracer, by chance, ended up near the sea surface

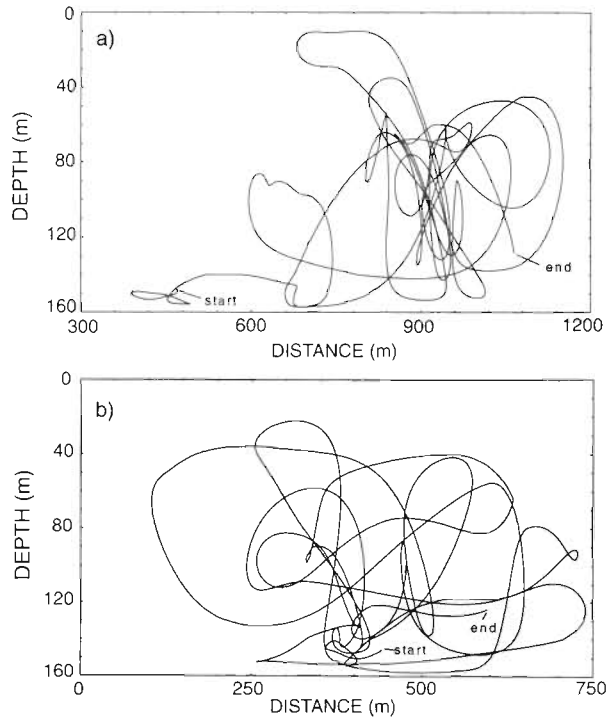

Fig. 10. Orbital motions of 2 selected Lagrangian tracers (a,b). Tracer positions sub-sampled every 10 min during 100 h of simulation starting at Day 16.5 in Expt FJORD 1990

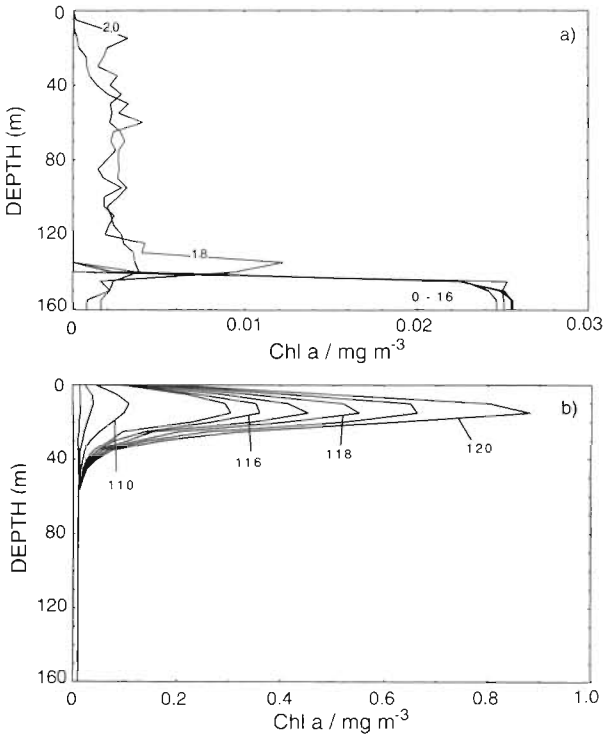

Fig. 12. Predicted evolution of chlorophyll *a* concentration (mg m^{-3}) for Expt FJORD 1990. (a) Simulation time: 0 to 20 d; (b) simulation time: 100 to 120 d

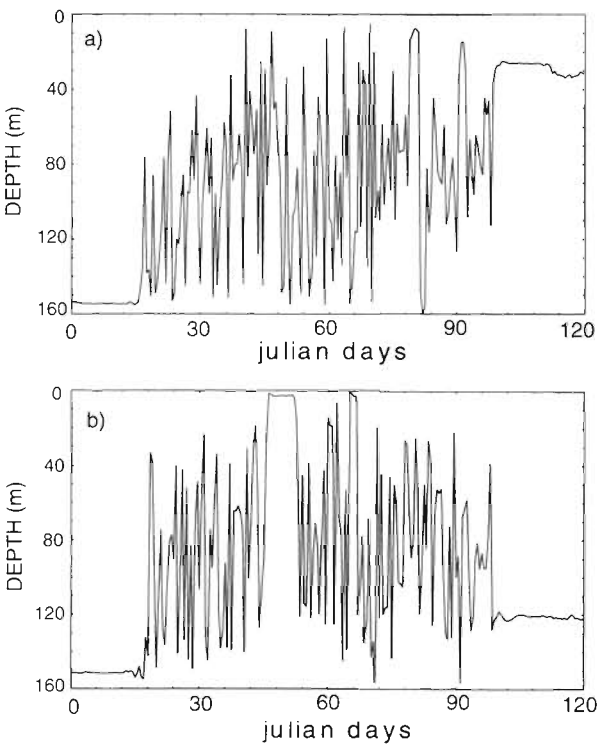

Fig. 11. Time series of vertical motions of 2 tracers randomly selected from the ocean slice for entire Expt FJORD 1990. (a) Tracer ends up near surface; (b) tracer ends up at depth

(Fig. 11a). The second, however, ended up at depth, far away from the euphotic zone (Fig. 11b).

Predicted primary production

The evolution of the phytoplankton stock for the winter/spring period of 1990 was characterised by slow production which, with light becoming available after about 30 d (cf. Fig. 3), lasted throughout the larger part of the simulation. Production commenced when tracers dispersed to the sea surface received light (cf. Fig. 9). Note that in this event spores become vegetative cells and the sinking velocity w_s changes from 120 m d^{-1} to 1 m d^{-1} in the PCM. Predicted concentrations increased very slowly throughout the water column (time >30 d), but stayed at values below 0.01 chl *a* (mg m^{-3}). The high initial concentration of plankton spores within the bottom layer (Fig. 12a) rapidly decreased between Days 14 and 18. This coincided with penetrative convection reaching the seabed (cf. Fig. 9). Thereafter, very low concentrations of spores were predicted (Fig. 12a) which, however, covered the entire water column. Note that initially the water column, apart from the bottom layer, was void of any plankton tracers. With the onset of a stable stratification (cf. Fig. 5b), i.e. after about 100 d of simulation, predicted plankton concentrations (Fig. 12b) showed a

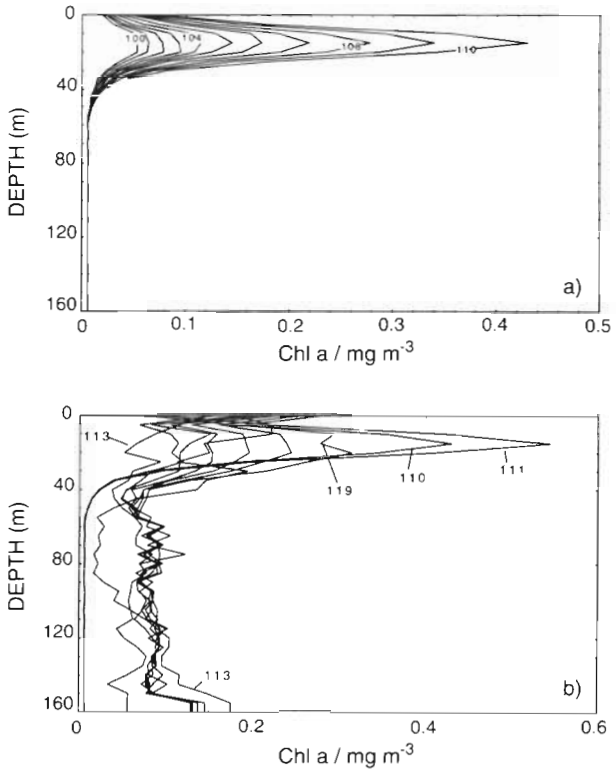

Fig. 13. Predicted evolution of chlorophyll *a* concentration (mg m^{-3}) for Expt FJORD 1994. (a) Simulation time: 100 to 110 d; (b) simulation time: 110 to 120 d

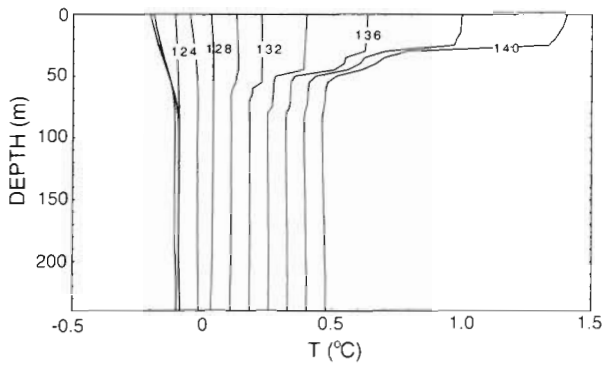

Fig. 14. Predicted temperature profiles (°C) for SHELF 1990. Simulation time: 120 to 140 d

rapid increase in the upper 40 m of the water column with a peak at depths around 20 m. Finally, at the end of the simulation (i.e. Day 120), predicted concentrations (Fig. 12b) arrived at a value of about 0.9 chl *a* (mg m^{-3}).

A very similar evolution of predicted production (Fig. 13) emerged from the FJORD 1994 run. However, one noteworthy difference occurred. After the development of a (weak) thermocline (cf. Fig. 6a), and a resulting increase in biomass (Fig. 13a), a convection event

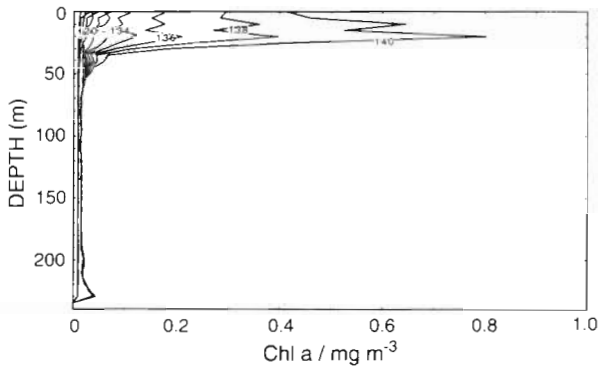

Fig. 15. Predicted evolution of chlorophyll *a* concentration (mg m^{-3}) for the end phase of Expt SHELF 1990. Simulation time: 120 to 140 d

accounted for a new homogenisation of the water column (cf. Fig. 6). As a result, vegetative plankton cells which had previously grown in the young thermocline were again distributed over the entire water column. Thereafter, the stratification stabilised again and a subsequent bloom occurred. Hence, plankton concentrations below 50 m (Fig. 13b) represented both plankton spores (concentrations: ~0.01 mg m^{-3}) and vegetative cells. The latter had concentrations which were higher by almost 1 order of magnitude (~0.1 mg m^{-3}).

Expt SHELF: Predicted stratification and primary production

Convective activity in Expt SHELF, as a result of higher oceanic heat losses for polar conditions (Fig. 4b), turned out to be more energetic compared to results of Expt FJORD. Nevertheless, very similar results in terms of both stratification and plankton production were obtained for this experiment. We confine the description of Expt SHELF to predicted plankton production in relation to the timing of the thermocline, allowing for a comparison with results of Expt FJORD. The onset of a seasonal thermocline (Fig. 14), emerging from a water column which was homogenised during the preceding winter, coincided with the start of a plankton bloom in spring (Fig. 15). The bloom was confined to the upper 40 m. Peak concentrations occurred around depths of 30 m. Note, that temperatures are much lower than in Expt FJORD. The slight warming of temperature profiles in Expt SHELF (cf. Fig. 14) was not the result of convection but the consequence of an additional positive heat flux which we prescribed throughout the water column. This way we simulated the effect of an advection of Atlantic heat with the Barents Sea inflow which, in the region considered, prevents the formation of sea ice.

DISCUSSION

According to general knowledge, oceanic convection in a global setting, i.e. the conveyor belt circulation (Broecker 1991), implies a sinking of water masses. However, conservation of mass requires that any sinking of water masses be compensated by an upward motion with the same magnitude in terms of water mass transport. As outlined in our synopsis, this upward convective motion is less energetic and it generally covers larger spatial scales than the more energetic downward motion.

In the context of primary production, according to our hypothesis, this less spectacular, weaker upward component of convection plays the most important role. Upward motion provides the mechanism which brings sinking phytoplankton spores towards the sea surface during winter. The presence of downward motions, occurring simultaneously in the vicinity of upward motions, disperses plankton throughout those parts of the water column which are affected by convection. In shallow, tidally dominated shelf seas, for instance in the North Sea, convective mixing in winter is supported by, or superimposed on, tidal mixing. Any observed mixed-layer deepening, for instance the formation of a perennial thermocline in the deep ocean, can only be explained by the existence of convection. In high and mid latitudes convection regularly destroys the seasonal thermocline in autumn and ventilates underlying waters during winter. This explains the reliability of the transport mechanism which we call phyto-convection.

The development of the phytoplankton spring bloom in northern Norwegian waters generally occurs in 2 critical phases. During the prebloom phase conditions for the subsequent bloom are set by providing the necessary inoculum of phytoplankton cells. In the bloom phase the actual growth takes place (Hegseth et al. 1995). In the latter a bloom dominated by spore-forming diatoms starts to develop during last part of March. At this time irradiance is sufficient to maintain growth in the euphotic zone (30 to 40 m), and day length has exceeded 12 h. In the prebloom phase, i.e. before the vernal equinox, few of the typical spring bloom species are found among the vegetative cells. Spores, however, have been found both in shallow and deep waters (Eilertsen et al. 1995). Very little increase in the phytoplankton biomass is registered in this early phase, which may be partly due to the photoperiodic dependence of spore germination. Most spores require a day length of at least 12 h to germinate (Eilertsen et al. 1995).

Sediments in fjords and coastal areas are found to contain up to 5 million spores ml^{-1} of diatom species (Eilertsen et al. 1995). Samples from the thin surface layer of the sediments function as a spring bloom inoculum under laboratory conditions at any time of the year (Hegseth et al. 1995). Hence, spores are a potential inoculum for any phytoplankton bloom under natural conditions, given that a sufficient amount could be brought up from the bottom sediments to the euphotic zone. This constitutes a critical phase in terms of the pre-conditioning of a plankton bloom.

Spores sink faster than vegetative cells (Davis et al. 1980, Bienfang 1981). Vegetative cells are able to regulate their buoyancy physiologically (Smayda 1970, Bienfang 1981). Spores with a large negative buoyancy must be maintained in the upper layers of a weakly stratified water column in early spring in order to allow for germination and subsequent growth. The maintenance of spores with negative buoyancy near the surface constitutes the second critical phase in primary production.

Both critical phases are explained by the predictions of our phyto-convection model. The results of the simulations are self-explanatory. They help us to understand why both vegetative plankton cells and spores can be present in the water column and, in particular, in the euphotic layer. The existence of both stages at the same time is a result of the randomness of convective dispersion. In spring, however, all cells within the water column have finally become vegetative. We arrived at this conclusion because the model predicted a weak growth during the preceding winter.

The randomness of phyto-convection, according to our modelling process study can be compared to a game of chance. This game is won by those vegetative plankton cells which, by chance, are within the euphotic layer at a time when convection finally ceases and a stable (though weak) stratification is built up. This is a result of both decreasing atmospheric forcing and increasing irradiance. A further establishment of the young thermocline may be disrupted by isolated atmospheric cooling events which frequently occur in spring. In this case convection again disperses plankton cells over the water column (cf. Fig. 13) and the gamble, governed by convective activity, commences again. Those cells which are within the euphotic layer after the cooling event would initiate a subsequent bloom. Hence, rapid weather changes in spring may induce a series of (little) blooms which eventually, with net warming, finally form a main bloom.

Observations of a series of 'brief' blooms preceding a main bloom are discussed in Townsend et al. (1994). These authors highlight the role of minor blooms in regard to carbon export and suggest that such blooms may considerably increase the estimated spring production as compared to (commonly applied) estimates based on just the main bloom. In this context it is interesting to note that also Niehoff et al. (1999) reported a

'pre-bloom' phase observed at Weather-ship M in the North Atlantic in 1997. It lasted for more than 1 mo and female copepodes (*Calanus finmarchicus*) produced as many eggs in the pre-bloom phase as in the following main bloom. Reported concentrations of phytoplankton during the pre-bloom phase were of a similar order of magnitude (~0.2 mg m^{-3}) as those predicted by our model.

The model predicted vegetative cells dispersed throughout the water column (Figs. 12 & 13). We, therefore, concluded that plankton beneath an established seasonal thermocline would sink very slowly. These cells may be lost for the respective production season. Given favourable (light and nutrient) conditions they might, however, later induce a secondary plankton bloom beneath the thermocline.

The predicted plankton dispersion within the water column (Fig. 9) showed an interesting feature during the first 40 h of simulation: tracers, which are spores at this time, do not reach the surface but are dispersed throughout the underlying water column. The surface layer, void of tracers, showed a thickness which was variable in time. This is explained by a competition between the sinking of spores and convective action. Once convection weakens as a consequence of variations in forcing, the sinking in relation to convective motions becomes more dominant (prescribed sinking rate was 120 m d^{-1}). The sinking affects all tracers in the water column, but it is only visible for those near the interface between the (clear) surface layer and underlying waters (cf. Fig. 9e,f). Once convective dynamics become strong enough as a result of both forcing and eroding stratification (time >40 d), tracers are also moved into the euphotic zone. Very near the sea surface (approximately in the upper 30 m) predicted vertical velocities of convection are generally smaller than at greater depth. Convective plumes first need to be accelerated before the sinking and, consequently also the rising of waters, attains higher speeds. Therefore, with weaker vertical velocities, it is easier to remove plankton cells from near-surface waters.

Provided there was enough light available for growth near the surface, the sinking rate of plankton in our model was reduced to 1 m d^{-1}. This simulates growing vegetative cells with a largely reduced negative buoyancy. However, the reduction only applies for cells which have been within the euphotic layer and which have received enough light for growth. It might be questionable to immediately change the sinking rate from 120 m d^{-1} to just 1 m d^{-1} once cells become vegetative. A slower transition might be a more appropriate description of changes in buoyancy as a consequence of vegetative growth. However, since a quantitative description of changes in sinking rates dependent on received irradiance was not available, we decided to simulate the transition in the rather crude manner described. A slower change in sinking rates would retard the vegetative growth of cells because they could be removed more frequently from the euphotic layer. The predicted growth until the onset of a seasonal thermocline was at any rate very small (cf. Figs. 11, 12 & 14) because growing cells were always removed from the euphotic layer by convective action. Therefore, the applied simulation of sinking rates has apparently very little influence on the final results of our simulations.

Typical predicted magnitudes of velocities in a developed convective regime are in the order of 1 to 10 cm s^{-1}. A (comparatively) large sinking rate of plankton of 200 m d^{-1} corresponds to a velocity of 0.23 cm s^{-1}. With this large difference between convective dynamics and sinking rates it is very likely that the vertical motions induced by convection will always override the effect of sinking. For that reason we did not carry out any further experiments with different sinking rates.

Applied to hydrographic conditions in a northern Norwegian fjord, and in the Barents Sea, the phyto-convection model was able to predict a dispersion of diatom spores from the seabed to surface layers, irrespective of the differences in water depth and stratification. It also predicted the following onset and growth of a phytoplankton bloom in a very weakly stratified water column, well before a well-developed seasonal thermocline (supported by melting of snow and ice, and freshwater run off) was established. The predicted young thermocline in early spring is characterised by a rather weak temperature contrast against underlying waters; it can be well below 0.1°K (cf. Figs. 5, 6 & 14). Apparently, even weak stability in the upper layers, particularly during daytime, is sufficient to support a bloom. Thermoclines of this scale are hard to detect in coarsely resolved CTD profiles. Consequently, they might have often been overlooked. However, the model results explain the observed start of phase 2 of the spring bloom. It takes place immediately after the reversal of the heat flux causes a net warming of the sea surface, which depends on local climate conditions (Hegseth et al. 1995).

Our model produced the results described above without any tuning. The available components, i.e. convection and Lagrangian phytoplankton model, were simply plugged together to form the coupled model. In the convection model the only parameter which could be modified, i.e. tuned, was the prescribed mixing length in the turbulence closure scheme. This, however, was set to a value which allowed for realistic simulations for the Greenland Sea. Hence, there was no reason to modify it because conditions in ambient turbulence in the Greenland Sea are

comparable with the cases considered here. In the Lagrangian phytoplankton model sinking rates dependent on light conditions and growth could be considered for a tuning. However, as outlined above, convective dynamics will eventually override these effects.

The mechanism of phyto-convection, here first described by process-oriented simulations of shallow water columns in high latitudes, worked reliably for different conditions in forcing, stratification and depth of water column. In order to highlight the fact that convection alone is able to play the anticipated role in plankton dispersion, dynamical support from tidal mixing was intentionally ignored. We believe that this fundamental mechanism also works in the deep open ocean in both high and temperate mid latitudes. In the open ocean phyto-convection would be confined to the perennial thermocline. With the absence of a seabed at shallow depths, where plankton can accumulate, we anticipate competition between sinking of phytoplankton and penetration speed of convection. This competition would determine the final success of a spring bloom. A cruise with the RV 'Valdivia' to the North Atlantic in spring 1999, and further model simulations for a deep oceanic water column, were devoted to an investigation of this extension of our hypothesis.

Acknowledgements. In this investigation we made use of model components which were developed with partial support from the Deutsche Forschungsgemeinschaft (DFG-SFB318) and the European Union (DG-XII, MAST II and III), within the European Sub-Polar Ocean Project (ESOP-1 and ESOP-2) (MAS2-CT93-0057 and MAS3-CT95-0015). We greatly acknowledge the help of Jennifer Verduin in editing our English.

LITERATURE CITED

Aagaard K, Carmach E (1989) The role of sea ice and other fresh water in the Arctic circulation. J Geophys Res 94 (C10):14485–14495

Aagaard K, Swift JH, Carmack EC (1985) Thermohaline circulation in the arctic mediterranean seas. J Geophys Res 90:4833–4846

Aksnes DL, Lie U (1990) A coupled physical-biological pelagic model of a shallow sill fjord. Estuar Coast Shelf Sci 31:459–486

Backhaus JO (1985) A three-dimensional model for the simulation of shelf sea dynamics. Dtsch Hydrogr Z 38:165–187

Backhaus JO (1995) Prozesstudien zur Ozeanischen Konvektion. Habilitationsabhandlung. Inst Meereskunde, Univ Hamburg (in German)

Backhaus JO, Kämpf J (1999) Simulations of sub-mesoscale oceanic convection and ice-ocean interactions in the Greenland Sea. Deep-Sea Res II 46:1427–1455

Backhaus JO, Wehde H (1997) Convection in the Baltic Sea—a numerical process study. In: Ozsoy E, Mikaelyan A (eds) NATO ASI-series: 'Sensitivity to change: Black Sea, Baltic Sea and North Sea' Kluwer Academic Publ, Dordrecht, p 295–309

Backhaus JO, Fohrmann H, Kämpf J, Rubino A (1997) Formation and export of water masses produced in Arctic shelf polynyas—process studies of oceanic convection. ICES J Mar Sci 54:366–382

Barkmann W, Woods JD (1996) On using a Langrangian model to calibrate primary production determined from *in vitro* incubation measurements. J Plankton Res 18: 767–788

Bienfang PK (1981) Sinking rates of heterogeneous, temperate phytoplankton populations. J Plankton Res 3:235–253

Billett DSM, Lampitt RS, Rice AL, Mantoura RFC (1983) Seasonal sedimentation of phytoplankton to the deep-sea benthos. Nature 302:520–522

Broecker WS (1991) The great ocean conveyer. Oceanography 4:79–89

Davis CO, Hollibaugh JT, Seibert DLR, Thomas WH, Harrison PJ (1980) Formation of resting spores by *Leptocylindrus danicus* (Bacillariopyceae) in a controlled experimental ecosystem. J Phycol 16:296–302

Degens ET (1968) Geochemie der Sedimente. Ferdinand Enke Verlag, Stuttgart

Dobson FW, Smith SD (1988) Bulk models of solar radiation at sea. Q J R Meterol Soc 114:165–182

Eilertsen HC, Taasen JP (1984) Investigations on the plankton community of Balsfjorden, northern Norway. The phytoplankton 1976–1978. Environmental factors, dynamics of growth, and primary production. Sarsia 6:1–15

Eilertsen HC, Sandberg S, Töllefsen H (1995) Photoperiodic control of diatom spore growth: a theory to explain the onset of phytoplankton blooms. Mar Ecol Prog Ser 116: 303–307

Friehe CA, Schmitt KF (1976) Parametrisation of air-sea interface fluxes of sensible heat and moisture by the bulk aerodynamic formulas. J Phys Oceanogr 6:801–809

Garrison DL (1981) Monterey Bay phytoplankton. II. Resting spore cycles in coastal diatom populations. J Plankton Res 3:137–156

Garrison DL (1984) Planktonic diatoms. In: Stridinger KS, Walker LM (eds) Marine plankton life cycle strategies. CRC Press, Boca Raton, FL, p 1–17

Gill AE (1982) Atmosphere ocean dynamics. Academic Press, San Diego, CA

Gran HH (1912) Pelagic plant life. In: Murray J, Hjort J (eds) The depth of the ocean. Cramer, Weinheim, p 307–386

Harms I (1994) Numerische Modellstudie zur winterlichen Wassermassentransformation in der Barents See. Berichte aus dem Zentrum für Meeres- und Klimaforschung Hamburg. Reihe B: 7

Harms I (1995) Water mass transformation in the Barents Sea—application of the Hamburg Shelf Ocean Model (HamSOM). ICES J Mar Sci 54:351–365

Hegseth EN, Svendsen H, von Quillfeldt CH (1995) Phytoplankton in fjords and coastal waters of northern Norway: environmental conditions and dynamics of the spring bloom. In: Skjoldal HR, Hopkins C, Erikstad KE, Leinaas HP (eds) Ecology of fjords and coastal waters. Elsevier Science BV, Amsterdam, p 45–72

Heimdal BR (1974) Composition and abundance of phytoplankton in the Ullsfjord area, North Norway. Astarte 7: 17–42

Holm-Hansen O, Lorenzen CJ, Holmes RW, Strickland JDH (1965) Fluorometric determination of chlorophyll. J Cons Perm Int Explor Mer 30:3–15

Jungclaus JH, Backhaus JO, Fohrmann H (1995) Outflow of dense water from Storfjord in Svalbard: a numerical model study. J Geophys Res 100(C12):24719–24728

Kämpf J, Backhaus JO (1998) Shallow, brine-driven free con-

vection in polar oceans: nonhydrostatic numerical process studies. J Geophys Res 103(C3):5557–5593
Kämpf J, Backhaus JO (1999) Ice-ocean interactions during shallow convection under conditions of steady winds: three dimenstional numerical studies. Deep-Sea Res II 46: 1335–1355
Kimball JF Jr, Corcoran EF, Wood EJF (1963) Chlorophyll containing microorganisms in the aphotic zone of the oceans. Bull Mar Sci 13:574–577
Kochergin VP (1987) Three-dimensional prognostic models. In: Heaps N (ed) Three-dimensional coastal ocean models Vol 4. Coastal Estuar Sci, Washington, DC, p 201–208
Malone TC, Falkowski PG, Hopkins TS, Rowe GT, Whitledge TE (1983) Mesoscale response of diatom populations to a wind event in the plume of the Hudson river. Deep-Sea Res 30:149–170
Mann KH, Lazier JRN (1991) Dynamics of marine ecosystems. Blackwell, Oxford
Marschall J, Schott F (1999) Open-ocean convection: observations, theory and models. Rev Geophysics 37:1–64
McCartney MS, Talley LD (1982) The Subpolar Mode Water of the North Atlantic Ocean. J Physical Oceanogr 12: 1169–1188
McCave IN (1986) Local and global aspects of the bottom nepheloid layers in the world ocean. Neth J Sea Res 20: 167–181
Moll A (1995) Regionale Differenzierung der Primärproduktion in der Nordsee: Untersuchungen mit einem dreidimensionalen Modell. ZMK Hamburg, Reihe B:19
Moll A (1998) Regional distribution of primary production in the North Sea simulated by a three-dimensional model. J Mar Syst 16:151–170
Niehoff B, Klenke U, Hirche HJ, Irigoien X, Head R, Harris R (1999) A high frequency time series at Weathership M, Norwegian Sea, during the 1997 spring bloom: the reproductive biology of *Calanus finmarchicus*. Mar Ecol Prog Ser 176:81–92
Normann U (1990) Hydrographical data report from northern Norwegian fjords and coastal areas. The Norwegian College of Fishery Science, Univ Tromsö (in Norwegian)
Normann U (1991) Hydrographical data report from northern Norwegian fjords and coastal areas. The Norwegian College of Fishery Science, Univ Tromsö (in Norwegian)
Normann U (1992) Hydrographical data report from northern Norwegian fjords and coastal areas. The Norwegian College of Fishery Science, Univ Tromsö (in Norwegian)
Normann U (1993) Hydrographical data report from northern Norwegian fjords and coastal areas. The Norwegian College of Fishery Science, Univ Tromsö (in Norwegian)
Passow U (1991) Species-specific sedimentation and sinking velocities of diatoms. Mar Biol 108:449–455
Pitcher GC (1991) Phytoplankton seed populations of the Cape Peninsula upwelling plume, with particular reference to resting spores of *Chaetoceros* (Bacillariophyceae) and their role in seeding upwelling waters. Estuar Coast Shelf Sci 31:283–301
Pitcher GC, Walker DR, Mitchell-Innes BA, Moloney CL (1992) Short-term variability during an anchor station study in the southern Benguela upwelling system: phytoplankton dynamics. Progr Oceanogr 28:39–64
Platt T, Subba Rao DV, Smith JC, Li WK, Irwin B, Horne EPW, Sameoto DD (1983) Photosynthetically competent phytoplankton from the aphotic zone of the deep ocean. Mar Ecol Prog Ser 10:105–110
Rudels B (1993) High lattitude ocean convection. In: Stone DB, Runcorn SK (eds) Flow and creep in the solar system: observations, modelling, theory. Kluwer Academic Publ, Dordrecht, p 323–356
Smayda TJ (1970) The suspension and sinking of phytoplankton in the sea. Oceanogr Mar Biol Annu Rev 8:253–241
Smetacek VS (1984) Role of sinking in diatom life-history cycles: ecological, evolutionary and geological significance. Mar Biol 84:239–251
Steele JH (1962) Environmental control of photosynthesis in the sea. Limnol Oceanogr 7:137–150
Townsend DW, Cammen LM, Holligan PM, Campbell DE, Pettigrew NR (1994) Causes and consequences of variability in the timing of spring phytoplankton blooms. Deep-Sea Res 41(5/6):747–765
van Aken HM, Becker G (1996) Hydrography and throughflow in the north eastern North Atlantic Ocean: the NANSEN project. Prog Oceanogr 18:297–346
von Bodungen B, von Bröckel K, Smetacek V, Zeitschel B (1981) Growth and sedimentation of the phytoplankton spring bloom in the Bornholm Sea (Baltic Sea). Kieler Meeresforsch Sonderh 5:49–60
von Quillfeldt CH (1996) Phytoplankton in fjords and coastal waters of northern Norway: species composition and succession. PhD thesis, Univ Tromsö
Wehde H (1996) Einfluß der Konvektion auf die Phytoplanktonentwicklung. Diplomarbeit, Inst Meereskunde Universität Hamburg (in German)

Editorial responsibility: Otto Kinne (Editor), Oldendorf/Luhe, Germany

Submitted: November 26, 1998; Accepted: June 4, 1999
Proofs received from author(s): October 28, 1999